Title: Dynamic hydrology and plant-mediated effects reduce greenhouse gas emissions and alter wetland microbial communities

Authors: Regina B. Bledsoe[a*] and Ariane L. Peralta[a]

Affiliations: [a]East Carolina University, Department of Biology, Greenville, NC, 27858, USA

Abstract

While wetlands represent a small fraction (~7%) of the world's land surface, it is estimated that one third of wetlands have been lost due to human activities. Wetland habitat loss decreases ecosystem functions such as improving water quality and mitigating climate change. These microbially mediated functions are dependent on particular soil redox conditions, which are altered by soil hydrology and the presence of plants. Differences in microbial physiology allow certain taxa (aerobes and facultative anaerobes) to adapt to fluctuating (dry/wet) hydrologic conditions, while other taxa (obligate anaerobes) are better adapted to continually saturated conditions. Therefore, the duration of hydrologic periods can affect soil microbial community structure and function. Further, plant-derived carbon, nutrients, and air are released by diffusion belowground which also impacts microbial activity in soils. In this study, we hypothesized that redox status due to continuous flooding would support greater abundance of microbial taxa involved in methanogenesis (obligate anaerobes), but plant-mediated oxygen transport would decrease methane emissions. Using a mesocosm design, we manipulated duration of hydrologic condition (i.e., stable dry, stable flooding, and alternating wet/dry) and presence of plants to induce soil redox changes in wetland soils. We measured soil redox status, used targeted amplicon sequencing to characterize the bacterial and archaeal communities, and measured greenhouse gas production to assess microbial function. Hydrology and to a lesser degree plant presence influenced

soil redox conditions. Hydrologic history strongly influenced microbial community composition, but plant presence and hydrologic treatment altered microbial function to a great degree. As predicted, plant presence decreased greenhouse gas production in the wetland mesocosms. While previous studies do not often include plants when assessing greenhouse gas emissions, this study highlights that plant-mediated decreases in greenhouse gas emissions are significant. If plant-mediated effects are not considered when estimating the carbon balance of ecosystems, then wetland carbon storage could be underestimated.

Introduction

Wetlands represent only 5-8% of terrestrial land surface (Mitsch et al., 2013); however, it is estimated that we have lost at least 33% of wetlands as of 2009 (Davidson et al., 2018). Loss of important functions is a consequence of land use conversion of wetlands to urban and agricultural development. These wetland ecosystems provide valuable services such as improving water quality by decreasing nutrient and pollutant loads and mitigating climate change by sequestering carbon. Therefore, there is an interest in conserving, restoring, and constructing wetlands for these ecosystem benefits. Examples of valuable wetland ecosystem functions are anaerobic microbial processes associated with saturated soils that promote complete inorganic nitrogen ($NO_3^- \rightarrow N_2$) removal via denitrification and suppress aerobic decomposition of organic matter. These same anoxic soil conditions can also support methane production (via methanogenesis), which could decrease long-term carbon storage and climate change mitigation benefits of wetlands. Microbial functions associated with delivery of ecosystem services have the potential to be managed to enhance beneficial wetland services (Peralta et al., 2014a). To achieve microbial management, a deeper understanding of the controls on wetland microbial ecosystem functions is needed.

In order to produce cellular energy, adenosine triphosphate (ATP), microorganisms catalyze a series of oxidative-reduction (redox) reactions. Aerobic respiration yields the greatest amount of energy and is expected under dry conditions but as water fills soil pore spaces, the soil matrix shifts to a reducing environment (Mitsch et al., 2013; Truu et al., 2009). Reducing environments favor anaerobic respiration in which other molecules such as nitrate, manganese, ferric iron, sulfate, and carbon dioxide are used as terminal electron acceptors (Burgin et al., 2011). As soil moisture increases, oxygen availability and soil redox potentials decrease , which corresponds to a shift in available electron acceptors (Truu et al., 2009). Redox potentials measured between +600 and + 250 mV are considered oxidative conditions while redox potentials measured from +250 to -400 mV are considered reducing

conditions (Truu et al., 2009). Therefore, measuring soil redox potential is useful for predicting which biogeochemical processes are likely to be carried out by soil microbes.

In order to manage microbial functions in support of nitrogen removal and retention but with decreased methane production, a better understanding of the extent that the presence of vegetation and changes in hydrology (e.g., flooding, drying) affect microbial communities is needed. Complex interactions between abiotic factors, such as soil physicochemical properties, redox status and nutrient availability, and biotic factors, including abundance of vegetation and microbial community structure, influence microbial functions to varying degrees. A microbial community is composed of many taxa with varying physiologies which respond differently to changes in the local environment (Mentzer et al., 2006; Nygaard and Ejrnæs, 2009). Particular microbes may be more adapted to specific hydrologic conditions in their environment, where only a subset of microbial taxa can persist in response to frequent changes in soil moisture (Peralta et al., 2014b; Truu et al., 2009). However, unexpected microbial responses can also occur due to dormancy of soil bacterial taxa (Lennon and Jones, 2011; Rocca et al., 2015). As such, hydrologic changes in wetlands due to drought, draining, and re-wetting cause shifts in soil redox potentials and microbial community composition and metabolism, which can influence the relative rates of anaerobic processes such as denitrification and methanogenesis (Kim et al., 2008; Peralta et al., 2014b; Truu et al., 2009).

If drying and re-wetting events are periodic, a cycle of activity and dormancy can maintain high microbial diversity compared to more stable environmental conditions (Peralta et al., 2014b). For example, denitrifiers are facultative anaerobes and are capable of using oxygen; but in anoxic conditions, denitrifiers can switch to reducing nitrate (NO_3^-) to nitrous oxide (N_2O) and dinitrogen (N_2) gas during respiration (Mitsch and Gosslink, 2007). In addition, methanogens are dominant in the most anoxic conditions such as flooded wetlands, and are responsible for converting carbon dioxide to methane gas (Mitsch and Gosslink, 2007). Fluctuating hydrologic conditions can shift the microbial

community to one that can only tolerate transitional zones. As hydrologic changes occur, anoxic-oxic interfaces provide environmental conditions that sometimes support methanotrophs that convert methane to carbon dioxide and denitrifiers (Conrad, 2009; McDonald and Murrell, 1997; Mitsch and Gosslink, 2007). Therefore, the availability of electron acceptor/s (e.g., oxygen, nitrate) in the soil environment influences the relative abundance of microbial functional groups (i.e., subset of microbes capable of using a suite of electron acceptors) and rates and types of microbial processes.

While hydrology is a primary determinant of soil redox potential, plants also modify the soil environment. The soil microenvironments that are in contact with plant roots are hotspots of microbial activity involved in transporting nutrients, oxygen, and carbon belowground (Chanton, 2005; Kuzyakov, 2010; Philippot et al., 2013). Plants can also transport methane aboveground through aerenchyma in shoots. Also, radial oxygen loss from plant roots can increase soil redox potentials around the root zone producing microenvironments that can support aerobic microbial processes (Chanton, 2005). Additionally, vegetation can alter soil redox potentials by facilitating transport of oxygen into roots zones (Chanton, 2005; Sundberg et al., 2007) and transporting methane from root zones into the atmosphere (Carmichael et al., 2014; Hu et al., 2015).

The aim of this study is to provide insight into how the duration of hydrologic change (i.e., dry, interim, wet), and the presence of vegetation in wetland soils change the structure of the microbial community, redox conditions, and greenhouse gas rates. We hypothesize that dry and dry/wet transition conditions will support similar microbial communities but that redox potentials and greenhouse gas rates will differ between manipulated hydrologic treatment conditions. We expect that dry conditions with and without vegetation will support higher redox potentials (i.e., oxidative conditions) and a higher rate of carbon dioxide production with some nitrous oxide production but little or no methane production. We expect this because dry and transition conditions should support similar communities of facultative anaerobes that can switch between respiration pathways depending on

current soil saturation levels. Additionally, in dry conditions soils are already aerated so plant-mediated gas transport belowground should not alter redox potentials. However, in fluctuating wet conditions, we expect that redox conditions will shift between oxidative and reducing conditions due to soil saturation. Also, the plant presence will increase redox potentials during saturated periods, due to plant-mediated gas transport belowground, compared to treatments where vegetation is absent. Due to lower oxygen levels when saturated conditions are present, we expect decreased carbon dioxide production but increased nitrous oxide production with plants and negative nitrous oxide rates without plants indicating incomplete or complete denitrification processes, respectively. Also, we expect methane production will be lower due to methanogens being obligate anaerobes. Flooded conditions will support different microbial communities than dry or fluctuating environments due to consistently low redox potentials (i.e., reducing conditions) resulting in the highest rates of methane production and complete denitrification rates since these are both anaerobic processes. Although, other studies (Carmichael et al., 2014; Hu et al., 2015) have found increased methane rates in the presence of some plant species, in the present study, we expect that soils with plants will have lower methane production compared to flooded soils without plants. This is expected due to oxygen transport from roots supporting aerobic methanotrophic microbial taxa that consume methane.

To test these hypotheses, we conducted a mesocosm experiment in which we manipulated hydrology (i.e., dry, interim, and wet) and presence of plants in wetland soils collected from with different hydrologic histories (i.e., dry, wet/dry transition, and saturated wet zones) of a restored coastal plain wetland. We measured soil nutrient concentrations, redox potentials, greenhouse gas concentrations, and characterized soil microbial communities using amplicon sequencing. By simulating acute differences in hydrologic states, the addition of plants, and maintenance of soil structure, we were able to link microbial-scale changes to ecosystem-level processes.

Methods

Study Site

We collected soil samples from the Timberlake Observatory for Wetland Restoration located in the Albemarle Peninsula in Tyrell County, North Carolina (35°54'22" N 76°09'25" W; Fig. 2.1). Previously described by Ardón et al., 2010 and Morse et al., 2012, the field site is part of the Great Dismal Swamp Mitigation Bank, LLC which is a 1,700 ha wetland consisting of 420 ha of mature forested wetland, 787 ha of forested wetland, 57.2 ha of drained shrub-scrub, and 440 ha of agricultural fields restored to wetland habitat in 2007 (Ardón et al., 2013, 2010). A major portion of the restoration effort was to remove drainage ditches and plant 750,000 saplings including *Taxidium distichm, Nyssa* spp., *Salix nigra, Fraxinus pennsylvania, and Quercus* spp. (Morse et al., 2012). A more recent survey indicates that the dominant plant species at the site is *Juncus effusus* L. along with *Euthamia caroliniana* (L.) Greene ex Porter & Britton, *Solidago fistulosa* Mill., and *Scirpus cyperinus* (L.) Kunth (Hopfensperger et al., 2014). The site is connected to the Albemarle Sound via the Little Alligator River, and the site's position in the landscape increases the potential for saltwater intrusion to occur. In addition, salinity in the sound ranges from 0-7 psu and up to 12 psu during drought years (Ardón et al. 2013). Even though there is little elevation change (-1 m to 2 m) across the restored wetland, there is a hydrologic gradient, which is driven by the position of the water table and represents upland dry, saturated wet, and transition dry/wet sites (Hopfensperger et al., 2014).

Mesocosm Experimental Design

We used a mesocosm approach to assess the changes in the soil microbial community, redox potentials, and greenhouse gas (GHG) production due to hydrologic changes and vegetation. We set up a mesocosm experiment using soil blocks collected from three sites within the Timberlake Observatory for Wetland Restoration field site. Soils were collected from the restored (12 years post-restoration)

portion of the site that was previously used as agricultural fields for several decodes prior to restoration (Ardón et al., 2010). We collected soils that represented three different hydrologic zones on the inflow side of the site at the following coordinates: 35°53'45.3"N 76°09'57.5"W (dry), 35°53'44.8"N 76°09'57.1"W (dry/wet transition or interim), and 35°53'44.3"N 76°09'56.0"W (wet). Six intact soil blocks (25 cm × 25 cm × 20 cm deep) were cut out from each of the three sites using landscaping knives and shovels. Soil history was determined by water table levels at the time of collection (dry=20 cm, interim=10 cm, and wet= 0 cm below surface level). Soil blocks were contained in dark plastic containers of the same dimensions as the soil blocks (Fig. 2.1). To manipulate hydrology within the mesocosm, vinyl tubing was inserted 3 cm from the bottom of the mesocosm container on each side and connected to a 1 L water bottle (Fig. 2.1). Water levels inside the mesocosm were maintained by filling the 1 L bottle to the desired height using rain water collected from a cistern. To manipulate the presence of vegetation, the mesocosm was divided in half and separated by root screen (20 µm stainless steel mesh). On one side plants were allowed to grow during the experiment, while the 'no plant' side was maintained by careful removal of above- and belowground plant biomass. Finally, 4" schedule 40 polyvinyl chloride (PVC) collars were inserted 5

cm below the surface as a sampling base for GHG chambers (described in subsection *GHG concentrations*). The mesocosm experiment was housed at the East Carolina University West Research Campus (Greenville, NC) under a covered hoop house with shade cloth which prevented precipitation and allowed 60% light into the hoop house. Soils were collected April 1, 2016, prepared on May 29, 2016, and experimental mesocosm sampling started on June 13, 2016 and ended on August 11, 2016. Temperatures ranged from 22.7°C ± 1.5 to 30.8°C ± 1.4 during the experimental sampling period.

Two weeks after installing PVC collars and setting up the plant treatment, we started hydrologic treatments. Hydrologic manipulation occurred over eight weeks to allow for multiple dry/wet transitions for the interim treatment. Mesocosms exposed to wet conditions were flooded by overhead watering

and maintained using water reservoirs filled to maximum container height (18 cm). Mesocosms exposed to dry conditions were maintained at a 5 cm water level. The dry/wet (interim) treatments fluctuated between flooded and dry conditions, as described above, every two weeks starting with a wet treatment and ending with a dry treatment. We measured soil redox status and microbial community composition at the beginning and end of the 8-week experiment. In addition, we measured GHG fluxes every two weeks starting two weeks after initiating hydrologic treatments. Finally, at the end of the eight week experiment, we collected soils for physiochemical analyses: soil moisture, pH, total carbon, total nitrogen, extractable ammonium and nitrate, phosphorus, potassium, magnesium, sulfur, iron, manganese, and organic matter concentrations (described in subsection *Soil Physiochemical Characteristics*).

Soil Redox Potentials

We measured soil redox status at the beginning and end of the hydrologic experiment using Indicator of Reduction in Soils (IRIS) tubes (InMass Technologies; (Jenkinson and Franzmeier, 2006) (Fig. S2.1A). The IRIS tubes are constructed from 1/2" schedule 40 PVC pipe coated in iron oxide (Fe (III)) paint (Rabenhorst, 2008). When exposed to oxidative conditions, Fe(III) is visible as an orange-red paint; but when exposed to anoxic conditions, Fe(III) is reduced to Fe(II) which dissolves in solution and appears as a clearing (white) on the tube (Jenkinson and Franzmeier, 2006; Rabenhorst, 2008). At the beginning of the experiment, two IRIS tubes (12 cm depth) were installed in each mesocosm: one on the plant side and one on the bare soil side. The IRIS tubes were incubated in mesocosm conditions for two weeks before removal and analysis. After we removed the IRIS tube, a non-coated PVC pipe was used to fill the hole. Two weeks prior to the end of the experiment, the non-coated PVC pipe was removed and replaced with a new IRIS tube to measure soil redox status at the end of the experiment.

We quantified the surface area of Fe(III) paint removed from IRIS tubes using ImageJ software (v1.48, (Schneider et al., 2012)). First, we imaged the entire tube by taking four pictures and then stitched the photo into a composite using GIMP2 (v2.8.14, https://gimp.org/) photo editing software. Next, we identified areas of artificial paint removal, that is scratches from installing or removing tubes, and manually filled these pixels. Then, using ImageJ software (v1.48, (Schneider et al., 2012)), we converted all colored pixels to black. We compared the number of white pixels to total pixels to determine the percent of paint removed. Interpretation of redox status is based on the percent paint removed from a 10 cm section of tubing and summarized as follows: 0% not reducing, 1-5% probably not reducing, 5-10% possibly reducing, 10-25% and >25% definitely reducing (Rabenhorst, 2008).

Greenhouse Gas (GHG) Concentrations

We examined the effects of hydrology and vegetation on GHG production. We measured GHG concentrations on June 13, 2016, two weeks after hydrologic treatments were established, and then every two weeks until August 11, 2016 for a total of five sampling events. The GHG collection chambers were 20 cm in height with a diameter of 8.25 cm and constructed from clear acrylic tubing. Since GHG samples were captured using clear chambers versus opaque chambers, GHG measurements represent total GHG fluxes and not just soil respiration due to microbial activity. Chambers were sealed on one end with silicon and a pipe cap with 33 mm septa installed as gas sampling port. At the time of sampling, chambers were placed on top of preinstalled PVC collars and the seal taped to prevent diffusion from the seam (Hoffmann et al., 2018). We collected gas samples every 30 minutes for a total of four time points. To collect gas samples, we used a needle attached to a 20 mL syringe, mixed headspace gas three times by pulling and depressing the plunger, and then collected 20 mL of sample. The collected gas sample was equally distributed between two 3 mL glass Exetainer vials (Lampeter, Wales, UK) fitted with screw top and dual layer septa. Samples were stored upside down at room temperature in a dark

location and were analyzed within 96 hours of collection. We analyzed GHG concentrations using a Shimazdu gas chromatograph (GC-2014) fitted with an electron capture detector to detect nitrous oxide and flame ionization detector with methanizer to measure methane and carbon dioxide. Calibration standards for June 13 and June 28, 2016 contained 0, 120, 240, 360, 480, and CO_2 ppm; 0, 1, 2, 3, 4, and 5 CH_4 ppm; and 0, 0.2, 0.4, 0.6, 0.8, and 1 N_2O ppm. Calibration standards for July 11, Jul 25, and August 11, 2016 contained 0, 120, 480, 1200, 2400, and 3000 CO_2 ppm; 0, 1, 4, 20, 40, and 50 CH_4 ppm; and 0, 0.2, 0.8, 20, 40, and 50 N_2O ppm. If a sample measured above the calibration curve, we diluted the sample and reanalyzed it.

We used the linear change in concentration and the ideal gas law to calculate GHG fluxes (Millar et al., 2018). However, upon curation of analyzed gas samples for GHG flux calculations, we identified that 30-50% of samples from no plant treatments were not linear and that 50-75% of those samples represented wet treatments. Due to the statistical power lost in determining the effects of hydrology and plants on GHG rates by removing these samples from further analyses, we chose an alternate approach to analyzing gas samples. We determined the concentration of CH_4, CO_2, and N_2O in each sample for the first sampling time point which occurred at the first 30 minute collection interval.

Bacterial and Archaeal Community Analyses

We assessed the soil microbial community composition at the beginning of the experiment ('start' based on soils collected from the IRIS tube installation) and at the end of the experiment ('final' based on soils collected during destructive sampling). We collected 'final' soil samples using a standard soil probe (3 cm diameter, 10 cm deep) from the same location that we collected GHGs samples. We extracted genomic DNA from soils using the Qiagen DNeasy PowerSoil Kit and diluted DNA to 20 ng μl^{-1}. This genomic DNA was used as template in PCR reactions and used barcoded primers (bacterial/archaeal

515FB/806R primer set) originally developed by the Earth Microbiome Project (Caporaso et al., 2012) to target the V4 region of the bacterial 16S subunit of the ribosomal RNA gene (Apprill et al., 2015; Caporaso et al., 2012; Parada et al., 2016). For each sample, three 50 µL PCR libraries were prepared by combining 35.75 µL molecular grade water, 5 µL Amplitaq Gold 360 10x buffer, 5 µL $MgCl_2$ (25 mM), 1 µL dNTPs (40mM total, 10mM each), 0.25 µL Amplitaq Gold 360 polymerase, 1 µL 515 forward barcoded primer (10 µM), 1 µL 806 reverse primer (10 µM), and 1 µL DNA template (10 ng μL^{-1}). Thermocycler conditions for PCR reactions were as follows: initial denaturation (94 °C, 3 minutes); 30 cycles of 94°C for 45 seconds, 50 °C for 30 seconds, 72 °C for 90 seconds; final elongation (72 °C, 10 minutes). The triplicate 50 µL PCR libraries were combined and then cleaned using the AMPure XP magnetic bead protocol (Axygen, Union City, California, USA). Cleaned PCR product were quantified using QuantIT dsDNA BR assay (Thermo Scientific, Waltham, Massachusetts, USA) and diluted to a concentration of 10 ng μL^{-1} before pooling libraries in equimolar concentration of 5 ng μL^{-1}. We sequenced the pooled libraries using the Illumina MiSeq platform using paired end reads (Illumina Reagent Kit v2, 500 reaction kit) at the Indiana University Center for Genomics and Bioinformatics Sequencing Facility.

Sequences were processed using the mothur (v1.42.0) (Schloss et al., 2009) (Schloss et al. 2009) MiSeq pipeline (Kozich et al., 2013). We assembled contigs from the paired end reads, quality trimmed using a moving average quality score (minimum quality score 35), aligned sequences to the SILVA rRNA database (v132) (Quast et al., 2013), and removed chimeric sequences using the VSEARCH algorithm (Rognes et al., 2016). We created operational taxonomic units (OTUs) by first splitting sequences based on taxonomic class and then binning into OTUs based on 97% sequence similarity. Taxonomic identity was assigned using the SILVA rRNA database (v132) (Quast et al., 2013).

Soil Physiochemical Characteristics

Soil proprieties were determined from soils collected during the destructive sampling of mesocosms at the end of the experimental duration. We collected six soil cores (3 cm diameter, 10 cm depth) from each side of the box (i.e., plant and no plant) and combined cores collected from one side into a composite sample (i.e., one plant composite and one no plant composite), passed soils through a 4 mm sieve, and homogenized samples prior to subsampling for soil analyses. For each sample, we measured gravimetric soil moisture by drying 20-30 g of field-moist soil at 105 °C for at least 24 hours. Approximately 5 g of field moist soil was extracted with 45 ml of 2 M KCl, and extractable ammonium (NH_4^+) and nitrate (NO_3^-) ions were colorimetrically measured using a SmartChem 200 auto analyzer (Unity Scientific Milford, Massachusetts, USA) at the East Carolina University Environmental Research Laboratory. To determine total carbon and total nitrogen (TC, TN), a subsample of air-dried soil was finely ground and sieved through a 500 µm mesh, and analyzed using an elemental analyzer (2400 CHNS Analyzer; Perkin Elmer; Waltham, Massachusetts, USA) at the Environmental and Agricultural Testing Service Laboratory, Department of Crop and Soil Sciences, North Carolina State University). A second subsample of air-dried soil was sent to Waters Agricultural Laboratories, Inc. (Warsaw, NC) and analyzed for pH, phosphorus, potassium, magnesium, sulfur, manganese, iron, and humic matter, using standard Mehlich III methods (Mehlich, 1984; Mylavarapu et al., 2014).

Statistical Analyses

All statistical analyses were performed in the R statistical environment (RStudio v1.2.5001, Rv3.6.1) (R Core Team, 2019). Prior to multivariate statistical analyses, we normalized sample-to-sample variation in sequence depth by taking the relative abundance of each OTU and dividing by the total number of OTUs for each soil community. We examined beta diversity by visualizing bacterial community responses to hydrologic history (field conditions) and hydrologic treatment (contemporary

dry/wet treatments) using principal coordinates of analysis (PCoA) of bacterial community composition based on Bray-Curtis dissimilarity. We used permutational multivariate analysis of variance (PERMANOVA) to determine differences between bacterial communities among hydrologic history, hydrologic treatment, and plant presence. Hypothesis testing using PERMANOVA was performed using the *vegan::adonis* function (Oksanen, 2015). Unique taxa representing each hydrologic history were determined by Dufrene-Legendre indicator species analysis using the *labdsv::indval* function (Roberts, 2016). Finally, soil parameters were compared against bacterial community patterns (based on Bray-Curtis dissimilarity) using *vegan::envfit* function (Oksanen, 2015). Soil parameters with $p<0.05$ were represented on the PCoA plot as vectors scaled by their correlation to microbial community patterns.

We constructed linear mixed effects models with sampling plot and sampling date as random effects to determine the importance of the fixed effects of hydrologic history (field conditions), hydrologic treatment (contemporary dry/wet treatments), and plant presence on GHG concentrations using the *lme4* R package (Bates et al., 2015). Then, we used AICc model comparisons, which adjust for small sample size, against the null model to determine which simplest combination of fixed effects (hydrologic history, hydrologic treatment, and plant presence) is needed to explain the most variation in GHG concentrations (Gorsky et al., 2019; Hurvich and Tsai, 1993). We compared individual fixed effects and the combination of those fixed effects. We did not use the interaction between the fixed effects hydrologic history and hydrologic treatment because we only had a sample size of n=2 for each group. Lastly, to determine the proportion of variance explained by fixed effects (marginal) and the complete model (conditional), we used the *MuMIn* R package (Barton, 2019; Gorsky et al., 2019). The CH_4, CO_2, and N_2O concentrations were log transformed to better meet normality assumptions prior to running mixed effects models. To assess microbial community structure and function relationships, we examined the relationship between individual GHG concentration to microbial community Bray-Curtis dissimilarity matrix using distance-based partial least squares regression in the *dbstats* R package (Boj et al., 2017).

Finally, we used Mantel R statistic function in the *vegan* R package (Oksanen, 2015) to examine the relationship between the soil properties (redox, moisture %, pH, ammonium, total soil C, phosphorus ppm, potassium ppm, magnesium ppm, sulfur ppm, and humic matter percent) and microbial community composition. Only soil properties with a correlation of <50% were used in the this analysis.

Results

Characterization of Soil Physical-Chemical Properties

There was little variability in soil properties across main effects (hydrologic history, hydrologic treatment, plant presence). However, there were notable differences in soil moisture between plant treatments within dry and wet hydrologic treatments. In addition, NO_3^- concentrations were below detection limits in samples with plants, but were measureable in samples without plants (0.01 ± 0.0005 to 0.25 ± 0.38 NO_3^- mg L^{-1}) (Table 2.1). Soil redox status as measured by IRIS tube analysis revealed that soils experiencing dry and interim treatments (0% iron oxide paint removed) were not reducing, while soils in wet treatments were reducing (average 40%, range 27-67% paint removed). In wet treatments, plant presence decreased soil redox status to a lesser degree (average 38%, range 27%-60% paint removed) than when plants were absent, but soils were still considered reducing (Fig. 2.2, Fig. S2.1).

Plant and Soil Redox Effects on Greenhouse Gas Concentrations

Methane (CH_4)

Within no-plant treatments, wet (19.9 ± 42.0 mg CH_4-C m^{-2}, average ± SD) and interim (6.5 ± 25.4 mg CH_4-C m^{-2}) hydrologic treatments produced the highest CH_4 concentrations and the greatest

variability between samples compared to dry treatments (0.22 ± 0.93) (Fig. 2.4). However, treatments with plants produced the lowest CH_4 concentrations across wet, dry, and interim hydrologic treatments (0.64 ± 0.47, 0.17 ± 0.16, 0.60 ±0.85 mg CH_4-C m^{-2}, respectively) (Fig. 2.4). The model with hydrologic history, hydrologic treatment, and plant presence explained the most variation in CH_4 concentrations based on ΔAICc score of 0 and AICc weight of 0.45 (Table S2.1). The full model explained 32% of variation, while the fixed effect of hydrologic treatment explained 21% of the variation and plant and hydrologic history only explained 4% and 6%, respectively (Table S2.1).

Carbon Dioxide (CO_2)

Within no-plant treatments, dry (104.7 ± 37.4 mg CO_2-C m^{-2}), interim (58.1 ± 30.6 mg CO_2-C m^{-2}), and wet (42.3 ± 18.5 mg CO_2-C m^{-2}) hydrologic treatments produced the highest CO_2 concentrations compared to treatments with plants (35.1 ± 19.2, 29.5 ± 15.0, 24.9 ± 0.6 mg CH_4-C m^{-2}, respectively) (Fig. 2.5). The model with the interaction of hydrologic treatment and plant explained the most variation in CO_2 concentrations based on a ΔAICc score of 0 and AICc weight of 0.93 (Table S2.1). The fixed effect of plant explained 32% of the variation and hydrologic treatment explained 15% of variation while the interaction explained 52% of variation (Table S2.1).

Nitrous Oxide (N_2O)

The N_2O concentrations were near zero in all hydrologic and plant treatments (range: 0.05-0.15 mg N_2O-N m^{-2}) (Fig. 2.6). The model with hydrologic treatment and plant explained the most variation in N_2O concentrations based on ΔAICc score of 0 and AICc weight of 0.53 (Table S2.1). The full model

explained only 14% of variation, while the fixed effect of plant explained 10% of variation and hydrologic treatment explained 3% of variation (Table S2.1).

Relationship Between Soil Redox Conditions and GHG Concentrations

We used linear regression to examine the relationship between soil redox status and GHG concentrations. CH_4 had weak but significant positive relationship to redox status (R^2=0.26, p=0.001). This relationship improved after removing a wet/no plant sample that had unusually high CH_4 concentrations (R^2= 0.45, p<0.001). In addition, CO_2 concentrations had a weak but significant negative relationship with redox conditions (R^2=0.19, p=0.005), and N_2O concentrations were not significantly related to redox conditions (R^2=0.01, p=0.25).

Patterns in Microbial Community Composition

Sequencing efforts returned a total of 1,570,135 reads and 35,897 operational taxonomic units (OTUs) before removing low abundance sequences occurring less than 10 times or 0.01% in all samples. After removing low abundance sequences, 1,505,797 reads representing 7,026 OTUs were retained after filtering. Within OTUs prior to filtering, 15,582 of those OTUs occurred once and 5,536 occurred twice in all samples. All samples were rarefied to 23,528 reads since this was the lowest read count among all samples.

Bacterial and archaeal community composition clustered by hydrologic treatment within hydrologic history. Hydrologic history (along PCoA axis 1) explained 24.5% of variation in microbial community composition while hydrologic treatment (along PCoA axis 2) explained 10.6% of variation (Fig. 2.7). The PERMANOVA results indicate that hydrologic history (R^2=0.305, p=0.001) and hydrologic

treatment (R^2=0.110, p=0.002) explained variation in microbial community patterns (Table S2.2). In addition, sulfur concentrations were correlated to soil microbial communities from the wet hydrologic history, pH levels were correlated to microbial communities from the interim hydrologic history; and total soil C and manganese concentrations were correlated to microbial communities from the dry hydrologic history. Also, overall patterns in microbial composition and soil properties were significantly correlated (Mantel r= 0.32, p= 0.001).

Indicator species analysis of the top 2.5% OTUs (by relative abundance at a significance level of $p \leq 0.01$) revealed that 33 OTUs, 21 OTUs, and 39 OTUs represented dry, interim, and wet hydrologic histories, respectively. The bacterial phyla Acidobacteria (Gp1, Gp2, Gp3, and Gp6) (24%) and Proteobacteria (Alpha-, Beta-, Delta-, and Gammaproteobacteria) (30%) represented communities from dry hydrologic histories, while the bacterial phyla Acidobacteria (Gp1, Gp10, Gp3, and Gp7) (33%) and Proteobacteria (Alpha-, Beta-, and Deltaproteobacteria) (29%) represented communities from interim hydrologic histories. Soils from wet hydrologic histories were represented by Acidobacteria (Gp1, Gp2, Gp3) (38%) and Proteobacteria (Alpha-, Delta-, and Gammaproteobacteria (21%). Finally, microbial taxa putatively associated with methane cycling including the archaeal genera *Methanobacterium* and the bacterial genera *Methylocystis* and *Syntrophobacter* were unique to microbial communities from wet hydrologic histories.

Relationships Between GHG Concentrations, Microbial Community Composition, and Soil Properties

Microbial community composition explained more of the variation in GHG concentrations than do soil properties. Distance-based partial least squares regression revealed that microbial community composition explained 51.3%, 54.8%, and 48.6%, of variation in concentrations of CH_4, CO_2, and N_2O, respectively, based on components 1 and 2. However, distance-based partial least squares regression

revealed that patterns in soil properties only explained 30.0%, 31.6%, and 17.9%, of variation in concentrations of CH_4, CO_2, and N_2O, respectively, based on components 1 and 2.

Discussion

This study revealed that initial hydrologic conditions (compared to manipulated hydrology) strongly influenced microbial community composition more than function. Mesocosm soils for this study were collected from wet, dry, and interim hydrologic histories from a restored wetland. This difference in hydrologic history resulted in distinct microbial community patterns with wet hydrology being the most distinct compared to microbial communities from the dry and interim hydrology. Specifically, dry hydrologic histories were represented by taxa in the genera *Gaiella*, which are classified as strict aerobes (Albuquerque et al., 2011). Wet hydrologic histories were uniquely identified by bacterial and archaeal taxa putatively associated with methanogenesis, methanotrophy, and iron reduction. These microbial processes occur in low redox/low oxygen systems (Burgin et al., 2011). Microbes that are facultative anaerobes can shift between aerobic and anaerobic respiration based on soil redox conditions, therefore they can metabolically shift during dynamic soil hydrologic conditions. However, obligate anaerobes such as methanogens are sensitive to soil oxygen concentrations and desiccation (Fetzer et al., 1993). For example, in a study of peat bog layers, oxic subsurface layers contained more methanotrophs than methanogens which were found only in anoxic layers near the bottom of the bog (Lew and Glińska-Lewczuk, 2018). This suggests that hydrology is a strong determinant of oxygen availability in soils and that wet hydrologic histories best support microbial communities involved in anaerobic processes.

Plant and hydrologic treatment strongly affected microbial function, despite hydrologic history acting as a robust environmental filter on microbial community composition. Plants can influence GHG

rates by consuming CO_2 during photosynthesis, releasing CO_2 during respiration, aerating soils in contact with roots, and releasing labile C from roots which can stimulate microbial activity (Carmichael et al., 2014; Chanton, 2005; Luan and Wu, 2014). In the current study, soil redox status as visualized with IRIS tubes indicated that oxidative conditions existed near plant roots. This result suggests that plants are transporting oxygen belowground into soils. Regardless of hydrologic history, CH_4 concentrations were highest and CO_2 concentrations were lowest in soils experiencing the wet hydrologic treatment. However, soil undergoing fluctuating hydrologic treatments had similar GHG concentrations to soils experiencing dry hydrologic treatments. As such, the GHG concentrations were lower in all hydrologic treatments with plants. The reduction in CH_4 with plant presence is likely due oxygen radiation from plant roots providing methanotrophs with needed oxygen for methane consumption, thereby decreasing methane emissions (Chanton, 2005; Truu et al., 2009). The reduction in CO_2 emissions in the presence of plants is likely due to plant photosynthesis and plant uptake of atmospheric CO_2 from within the collection chamber (Luan and Wu, 2014). This suggests that plants are important mediators of GHG production in wetland soils. These results reveal that fluctuating soil moisture levels can decrease CH_4 emissions even within soils from wet hydrologic histories. Therefore, both hydrology of soils and plant presence are two important considerations when planning wetland restoration with the goal of enhancing soil C storage.

Results of this study highlight the importance of considering plant contributions to GHG emissions. Many studies investigating GHG emissions use opaque chambers to decrease heating of the headspace; however, these chambers can bias measurements of CH_4 emissions (Günther et al., 2014; Luan and Wu, 2014). Estimates of GHG emissions that do not include plant inputs can underestimate the C storage potential of wetlands. For example, a previous study estimates the C storage potential of wetlands by subtracting CO_2 sequestered from the atmosphere from CH_4 released from soils to determine that the world's wetlands sequester ~118 g-C m^{-2} $year^{-1}$ (Mitsch et al., 2013). However, it is

unclear if the studies used to estimate this value considered local soil hydrology and whether plants were present or not. According to our study and others (Günther et al., 2014; Luan and Wu, 2014), plant inclusion and plant species considerations in most cases would decrease the total estimation of CH_4 emissions from wetlands. These findings suggest that to improve estimations of C storage in wetlands, plant presence and hydrologic status should be considered in order to understand wetlands' potential to be a C sink.

Further, increasing extreme weather events cause changes in duration of decreased or excessive rainfall, which will alter microbial ecosystem functions. Changes in precipitation regimes could directly alter soil hydrology or plant abundance and composition. Results from this study reveal that the longer the duration of hydrologic change, the more dramatic the change in ecosystem functions. These results can be used to infer what might happen during an extreme drought event. One potential scenario is that during early summer a saturated non-tidal coastal plain wetland experiences decreased rainfall to the degree that the first meter of soil completely dries out and kills all vegetation. This may temporarily decrease methane emissions, but if in the following month the same area then becomes saturated again methane emissions could increase due to the lack of vegetation. However, if the duration of drying alters the microbial community structure, then methane production may be decreased upon re-flooding since obligate anaerobes will not persist under dry, aerated conditions. This warrants future studies to more closely examine the temporal component of when changes in hydrology permanently alter microbial community structure and lead to unexpected changes to ecosystem functions.

Acknowledgments

We thank J. LeCrone, L. Armstrong, M. Stillwagon, G. Gunderson, C. Eakins, (Joseph ???), and Chad Bledsoe for field and laboratory assistance. We thank J. Gill and the East Carolina University grounds crew for their efforts in maintaining grounds surrounding the shade house. This work

was supported by the National Science Foundation (GRFP to RBB) and East Carolina University.

All code and data used in this study can be found in a public GitHub repository (https://github.com/PeraltaLab/WetlandMesocosm_GHG_Timberlake) and the NCBI SRA (BioProject: PRJNA636184).

Figures and Tables

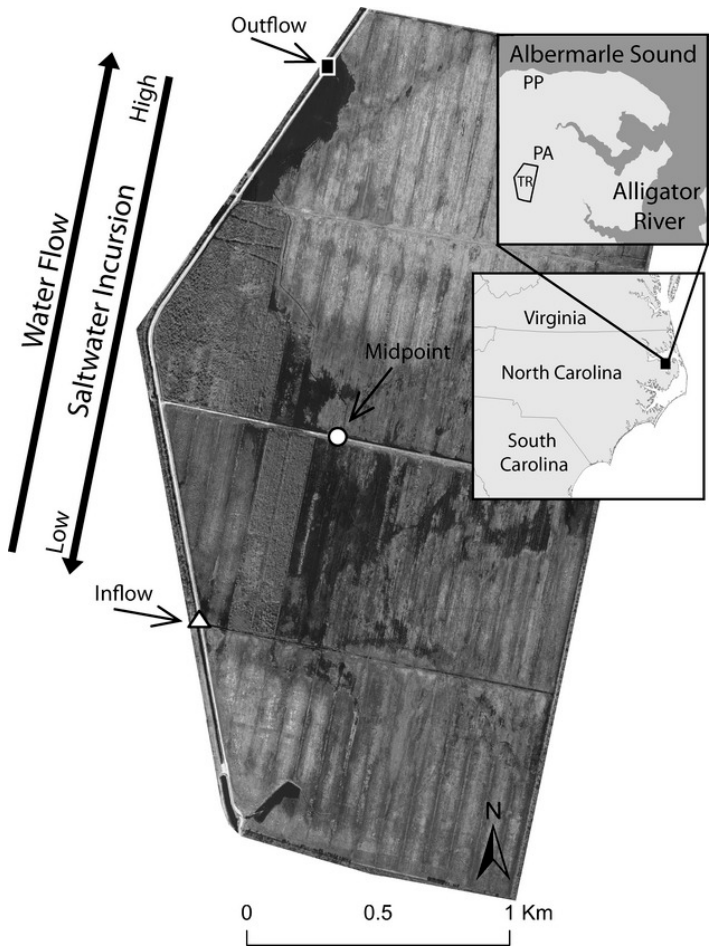

Figure 2.1. Timberlake Observatory for Wetland Restoration. (Modified from Ardón et al., 2013)

Figure 2.2. Mesocosm setup. Top: Left side of box represents plant treatment, and right side represents no plant treatment. There is a stainless mesh divider between each side. PVC collars permanently placed in mesocosm for GHG sampling. 1 liter bottle attached to each side of the mesocosm used to maintain water levels. Middle: Example of a wet treatment mesocosm with IRIS tubes installed. Bottom: Example of mesocosm with prepared for GHG sampling.

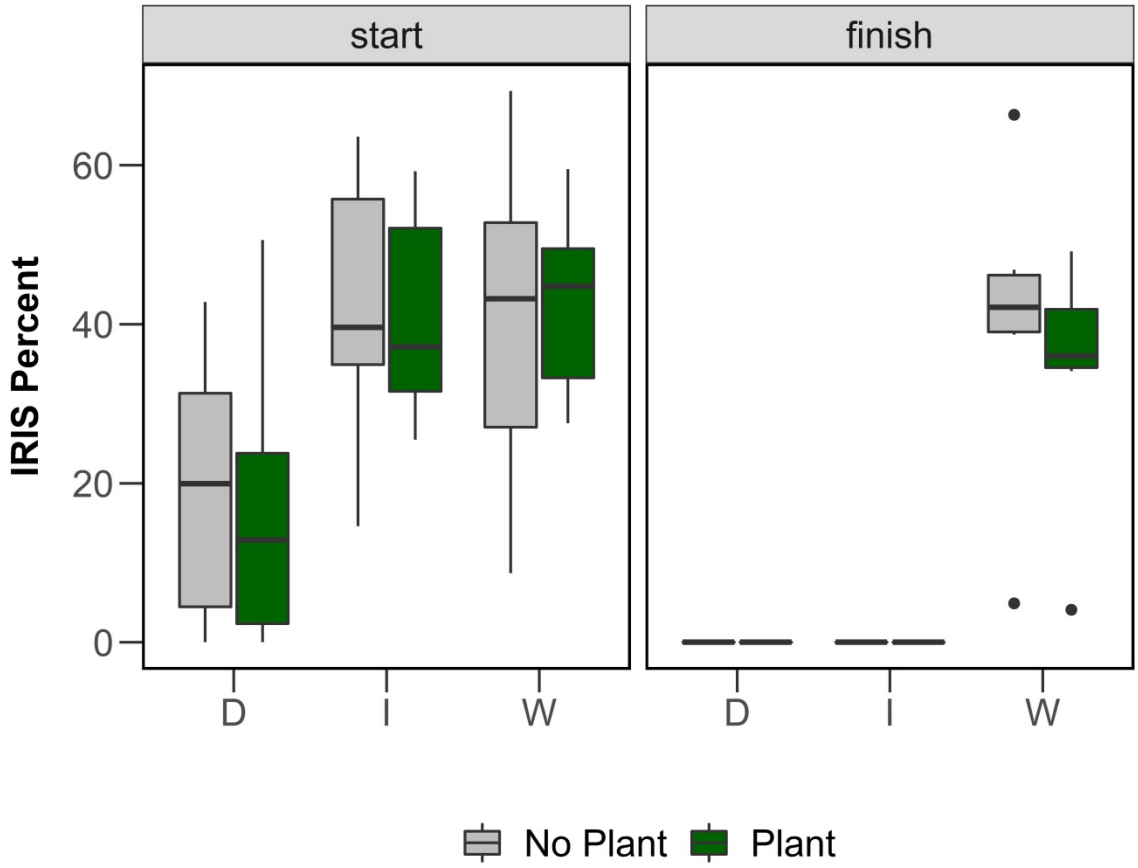

Figure 2.3. Boxplots of percent paint removed from IRIS tubes at start of experiment and the end of experiment. Note: At start of experiment plants were at seedling stand and fully mature by the end of experiment. D= dry, I=interim, W= wet. Gray= no plant, Dark green= plant present.

Table 2.1. Soil properties. Mean ± SD by hydrologic treatment and plant status. Abbreviations: MDL = Below detection limit.

	Dry		Interim		Wet	
	No Plant	Plant	No Plant	Plant	No Plant	Plant
Moisture %	39 ± 0.31	14 ± 0.03	19 ± 0.16	13 ± 0.02	29 ± 0.23	62 ± 0.07
pH	5.31 ± 0.11	5.31 ± 0.09	5.4 ± 0.16	5.35 ± 0.1	5.55 ± 0.15	5.41 ± 0.17
NH_4^+ mg/L	0.39 ± 0.07	0.27 ± 0.04	0.26 ± 0.1	0.19 ± 0.02	0.77 ± 0.76	0.39 ± 0.42
NO_3^- mg/L	0.08 ± 0.07	MDL	0.25 ± 0.38	MDL	0.01 ± 0.0005	MDL
C%	4.63 ± 0.78	4.63 ± 0.81	4.48 ± 0.32	4.37 ± 0.52	4.91 ± 0.92	4.68 ± 0.74
N%	0.22 ± 0.03	0.22 ± 0.03	0.22 ± 0.01	0.21 ± 0.03	0.24 ± 0.04	0.23 ± 0.03
P ppm	21 ± 4.14	20.41 ± 4.4	23.58 ± 8.87	22.83 ± 8.37	23.16 ± 5.98	23 ± 5.79
K ppm	33.66 ± 5.97	30.25 ± 10.31	39.5 ± 11.44	26.75 ± 3.04	46.16 ± 16.02	34.25 ± 10.78
Mg ppm	77.58 ± 6.46	74.66 ± 11.43	86 ± 22.33	78.66 ± 16.47	89.25 ± 16.85	79.41 ± 18.8
S ppm	15.75 ± 1.94	15.33 ± 2.29	13.25 ± 1.25	12.16 ± 0.4	11.33 ± 1.21	11.5 ± 1
Fe ppm	252.66 ± 14.45	243.66 ± 17.06	275.33 ± 27.07	251.16 ± 37.6	306.83 ± 22.52	280.66 ± 40.71
Mn ppm	3.91 ± 1.15	3.41 ± 0.97	4.33 ± 1.16	4.58 ± 1.31	5.83 ± 1.32	5.58 ± 2.05
Humic Matter%	2.35 ± 0.19	2.17 ± 0.14	2.04 ± 0.29	2.28 ± 0.22	1.98 ± 0.422	1.96 ± 0.43

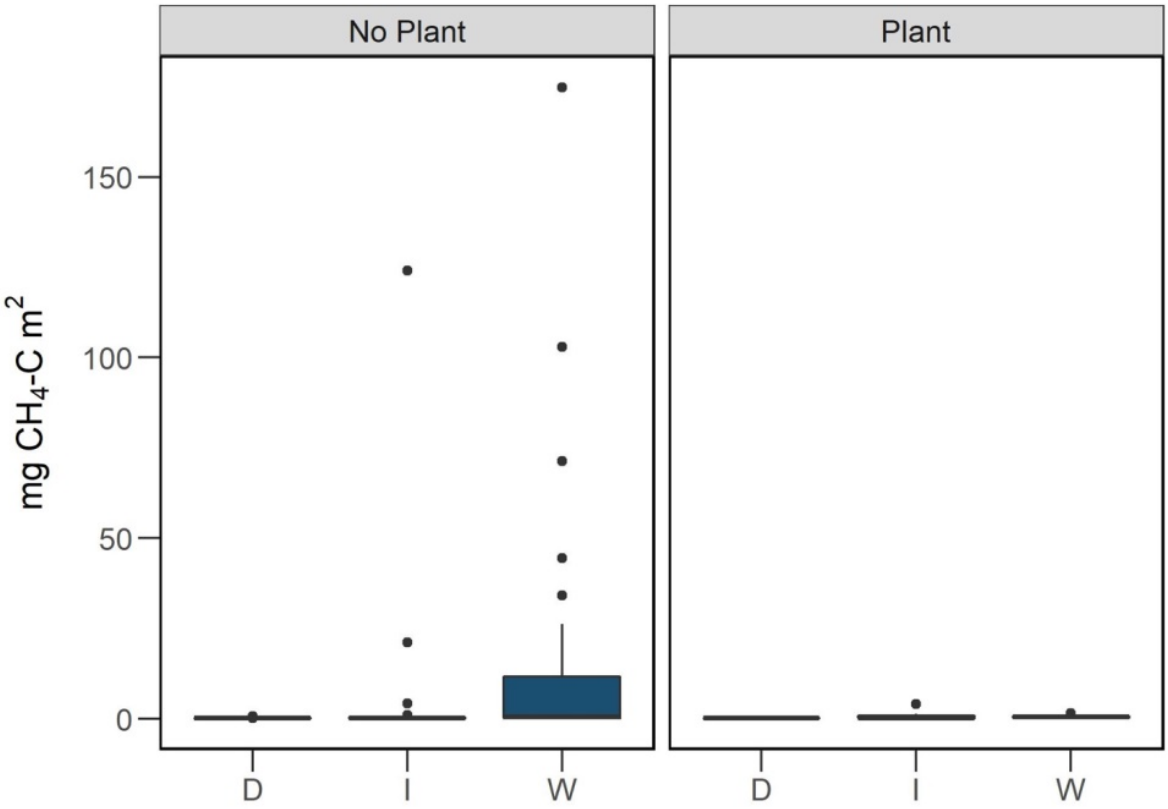

Figure 2.4. Boxplots of CH_4 concentrations by hydrologic treatment. Plot on left represents samples in no plant treatment and right represents plant treatment. D=dry, I= interim, W= wet.

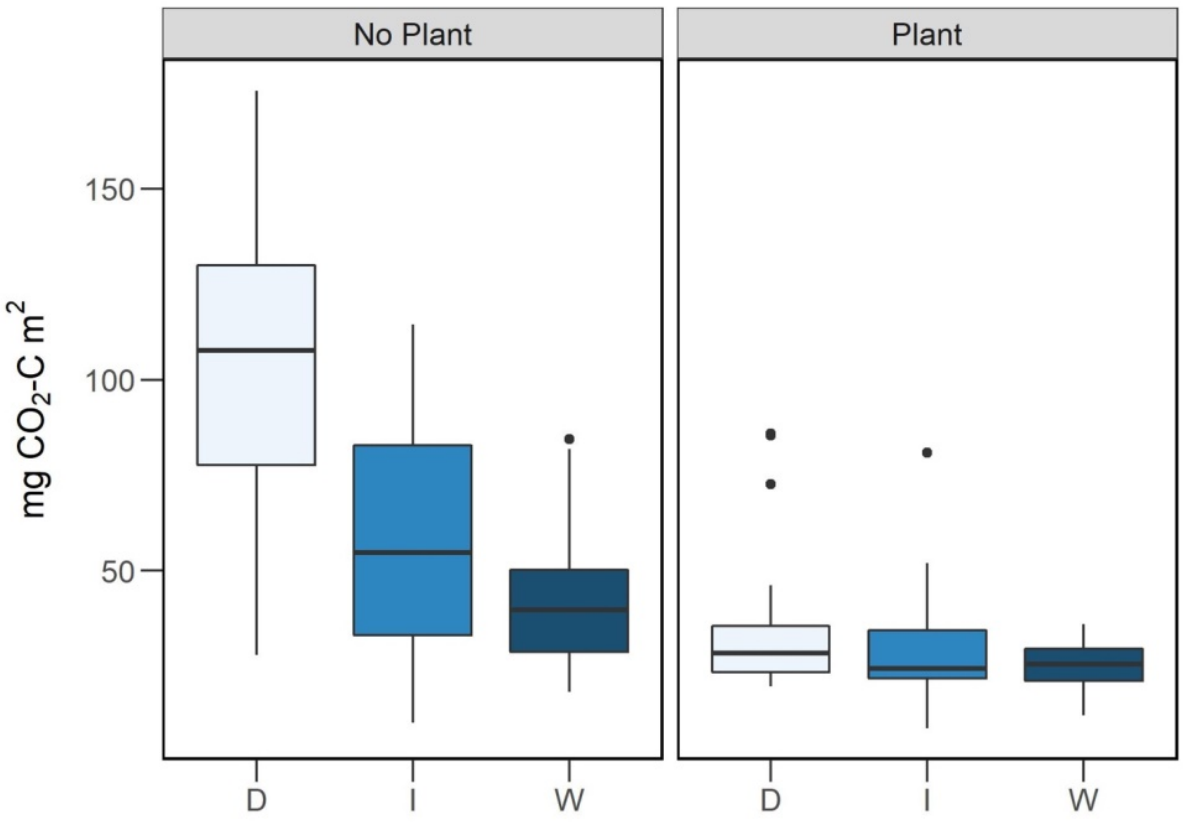

Figure 2.5. Boxplots of CO_2 concentrations by hydrologic treatment. Plot on left represents samples in no plant treatment and right represents plant treatment. D=dry, I= interim, W= wet.

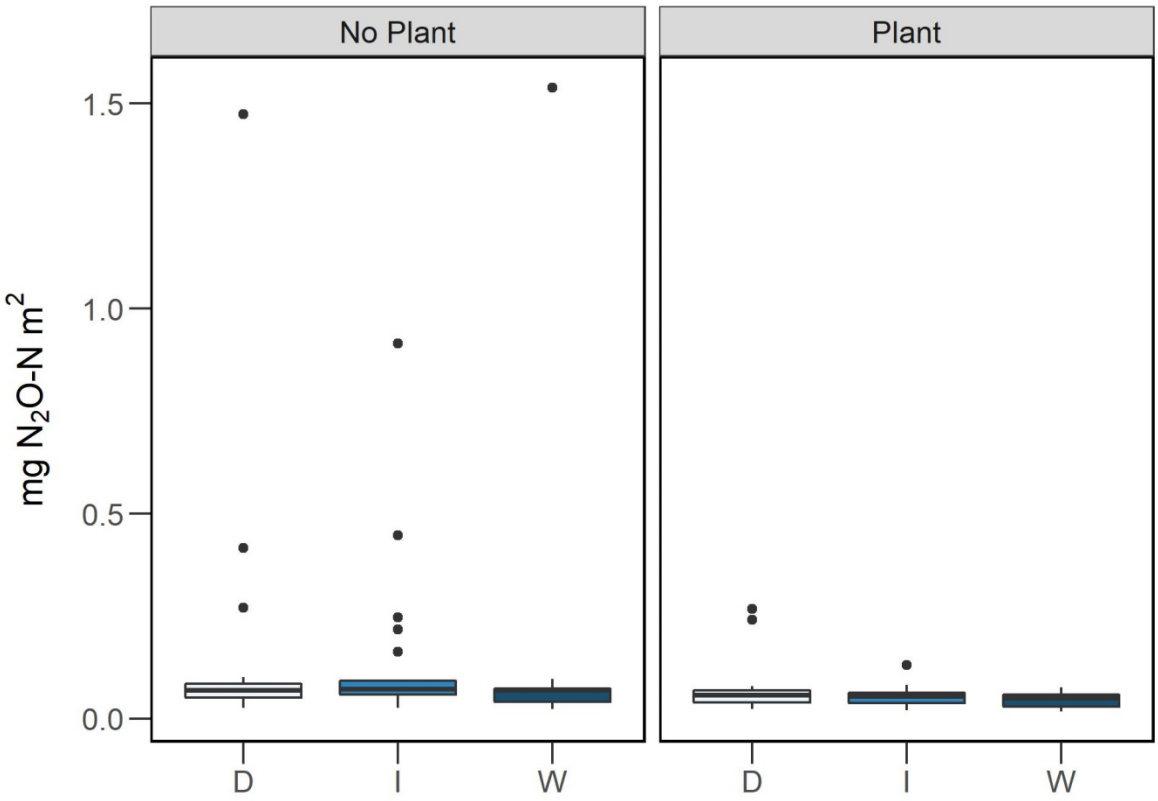

Figure 2.6. Boxplots of N_2O concentrations by hydrology treatment. Plot on left represents samples in no plant treatment and right represents plant treatment. D=dry, I= interim, W= wet.

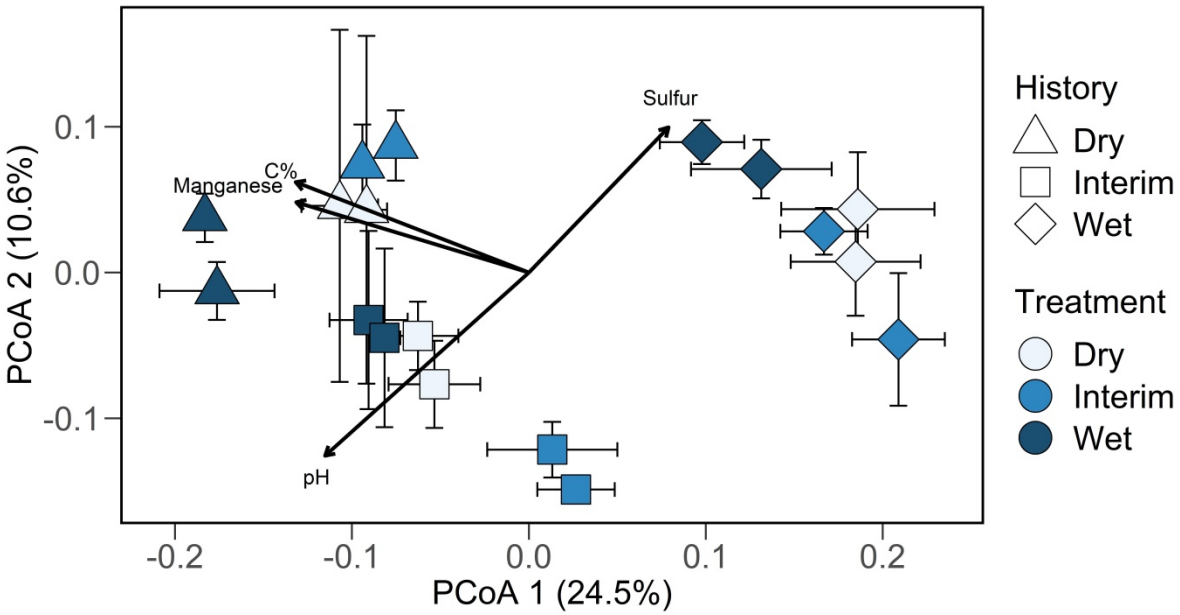

Figure 2.6. Ordination plot of PCoA analyses of bacterial and archaeal community composition based on Bray-Curtis dissimilarity matrix. Colors refer to hydrologic treatments white = dry, blue = interim, dark blue = wet. Shapes refer to hydrologic history of the sample: triangle = dry, square= interim, diamond = wet.

Supplemental Figures and Tables

Figure S2.1. Indicator of Reduction in Soils (IRIS) tubes. Representative IRIS tubes collected from the dry hydrologic treatment without plants (A.) and without plants (B), wet treatment without plants (C), in wet treatment with plants (D).

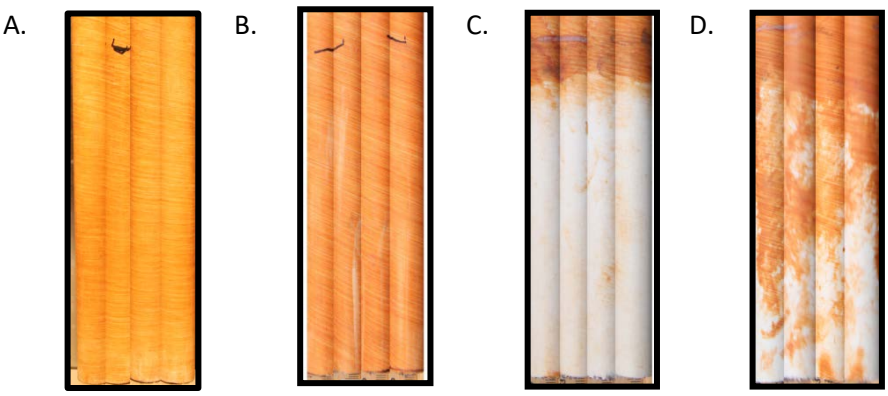

Table S2.1. Summary of mixed effects models to explain variation in greenhouse gas concentrations (CH_4, CO_2, N_2O) due to fixed effects of hydrologic history, hydrologic treatment, and plant presence and random effects of sample plot and date. Fixed effects: H = hydrologic history (dry, interim, wet), T = hydrologic treatment, and P = plant.

Model	k	AICc	ΔAICc	AICc Wt	R^2 Marg	R^2 Cond
CH_4						
P+T+H	9	455.64	0.00	0.45	0.32	0.60
P+T	7	457.25	1.61	0.20	0.26	0.60
T+H	8	457.63	1.98	0.17	0.28	0.60
	6	458.66	3.02	0.10	0.21	0.60
Treatment						
P*T	9	458.86	3.21	0.09	0.27	0.60
Plant	5	468.62	12.97	0.00	0.04	0.60
Null	4	468.84	13.20	0.00	-	0.60
P+H	7	469.19	13.54	0.00	0.10	0.60
History	6	469.61	13.96	0.00	0.06	0.60
P*T	9	470.51	14.87	0.00	0.27	0.60

CO_2						
P*T	9	184.92	0.00	0.93	0.52	0.60
P+T+H	9	191.00	6.08	0.04	0.50	0.60
P+T	7	191.95	7.03	0.03	0.48	0.60
Plant	5	210.43	25.51	0.00	0.32	0.60
H+P	7	212.05	27.13	0.00	0.35	0.60
H*P	9	215.29	30.37	0.00	0.36	0.60
	6	228.06	43.13	0.00	0.15	0.60
Treatment						
H+T	8	230.74	45.82	0.00	0.17	0.60
Null	4	233.27	48.35	0.00	-	0.60
History	6	236.25	51.33	0.00	0.02	0.60
N_2O						
P+T	7	290.27	0.00	0.53	0.14	0.22
Plant	5	291.59	1.32	0.27	0.10	0.19
T*P	9	293.95	3.68	0.08	0.14	0.23
P+T+H	9	294.17	3.91	0.07	0.14	0.23
H+P	7	295.39	5.12	0.04	0.11	0.19
P*H	9	299.90	9.63	0.00	0.11	0.20
	6	305.97	15.70	0.00	0.03	0.14
Treatment						
Null	4	306.12	15.85	0.00	-	0.14
H+T	8	309.92	19.65	0.00	0.03	0.14
History	6	310.00	19.73	0.00	0.00	0.14

Table S2.2. Summary PERMANOVA comparing microbial community composition due to main effects (plant, hydrologic history, hydrologic treatment) and interaction between plant × history and plant × treatment. Bolded text indicates significant differences.

Main Effect	SumSq	F-value	R^2	P-value
Plant	0.034	0.698	0.102	0.824
History	**0.743**	**7.562**	**0.305**	**0.001**
Treatment	**0.256**	**2.605**	**0.110**	**0.002**
Plant × History	0.066	0.667	0.027	0.942
Plant × Treatment	0.059	0.598	0.024	0.986

Table S2.3. Summary of bacterial and archaeal (OTUs) representative of hydrologic history based on indicator species analysis. These are the top OTUs (>2.5% relative abundance) that are significantly (p<=0.01) associated with dry, interim, and wet hydrologic histories.

OTU_ID	Cluster	IndVal	Prob	Classification Domain; Phylum; Class; Order; Family; Genus
Otu00082	dry	0.675	0.001	Archaea; Thaumarchaeota; Nitrososphaerales; Nitrososphaeraceae; Nitrososphaera; Nitrososphaera
Otu00225	dry	0.475	0.008	Bacteria; Acidobacteria; Acidobacteria Gp1;
Otu00048	dry	0.426	0.006	Bacteria; Acidobacteria; Acidobacteria Gp2;
Otu00081	dry	0.502	0.001	Bacteria; Acidobacteria; Acidobacteria Gp3;
Otu00010	dry	0.433	0.001	Bacteria; Acidobacteria; Acidobacteria Gp6;
Otu00014	dry	0.443	0.007	Bacteria; Acidobacteria; Acidobacteria Gp6;
Otu00055	dry	0.413	0.009	Bacteria; Acidobacteria; Acidobacteria Gp6;
Otu00111	dry	0.551	0.002	Bacteria; Acidobacteria; Acidobacteria Gp6;
Otu00151	dry	0.552	0.002	Bacteria; Acidobacteria; Acidobacteria Gp6;
Otu00096	dry	0.535	0.001	Bacteria; Actinobacteria; Actinobacteria;
Otu00163	dry	0.506	0.002	Bacteria; Actinobacteria; Actinobacteria; Actinomycetales;
Otu00090	dry	0.476	0.001	Bacteria; Actinobacteria; Actinobacteria; Gaiellales; Gaiellaceae; Gaiella
Otu00101	dry	0.418	0.003	Bacteria; Actinobacteria; Actinobacteria; Gaiellales; Gaiellaceae; Gaiella
Otu00035	dry	0.497	0.001	Bacteria;
Otu00128	dry	0.498	0.002	Bacteria;
Otu00175	dry	0.487	0.001	Bacteria;
Otu00176	dry	0.398	0.01	Bacteria;
Otu00114	dry	0.517	0.001	Bacteria; Bacteroidetes; Sphingobacteriia; Sphingobacteriales; Chitinophagaceae; Chitinophagaceae
Otu00071	dry	0.443	0.002	Bacteria; Bacteroidetes; Sphingobacteriia; Sphingobacteriales; Chitinophagaceae; Terrimonas
Otu00274	dry	0.449	0.009	Bacteria; Firmicutes; Bacilli; Bacillales; Bacillaceae 1; Bacillaceae 1
Otu00250	dry	0.501	0.002	Bacteria; Planctomycetes; Planctomycetia; Planctomycetales; Planctomycetaceae; Planctomycetaceae
Otu00001	dry	0.381	0.007	Bacteria; Proteobacteria; Alphaproteobacteria; Rhizobiales;
Otu00040	dry	0.423	0.002	Bacteria; Proteobacteria; Alphaproteobacteria; Rhizobiales;
Otu00161	dry	0.438	0.004	Bacteria; Proteobacteria; Alphaproteobacteria; Rhodospirillales;
Otu00104	dry	0.546	0.001	Bacteria; Proteobacteria; Alphaproteobacteria;

				Sphingomonadales; Sphingomonadaceae;
Otu00042	dry	0.528	0.001	Bacteria; Proteobacteria; Betaproteobacteria;
Otu00049	dry	0.535	0.001	Bacteria; Proteobacteria; Betaproteobacteria;
Otu00169	dry	0.440	0.007	Bacteria; Proteobacteria; Deltaproteobacteria; Myxococcales; Myxococcales; Myxococcales
Otu00153	dry	0.766	0.001	Bacteria; Proteobacteria; Gammaproteobacteria;
Otu00170	dry	0.659	0.001	Bacteria; Proteobacteria; Gammaproteobacteria;
Otu00198	dry	0.708	0.001	Bacteria; Proteobacteria;
Otu00186	dry	0.554	0.004	Bacteria; Verrucomicrobia; Spartobacteria;
Otu00242	dry	0.471	0.001	Bacteria; Verrucomicrobia; Subdivision3;
Otu00018	interim	0.466	0.001	Bacteria; Acidobacteria; Acidobacteria Gp1;
Otu00058	interim	0.412	0.005	Bacteria; Acidobacteria; Acidobacteria Gp1;
Otu00106	interim	0.619	0.001	Bacteria; Acidobacteria; Acidobacteria Gp10;
Otu00056	interim	0.459	0.003	Bacteria; Acidobacteria; Acidobacteria Gp3;
Otu00092	interim	0.515	0.001	Bacteria; Acidobacteria; Acidobacteria Gp3;
Otu00122	interim	0.468	0.001	Bacteria; Acidobacteria; Acidobacteria Gp3;
Otu00112	interim	0.457	0.001	Bacteria; Acidobacteria; Acidobacteria Gp7;
Otu00032	interim	0.481	0.002	Bacteria;
Otu00057	interim	0.485	0.006	Bacteria;
Otu00311	interim	0.729	0.001	Bacteria;
Otu00221	interim	0.522	0.001	Bacteria; Chloroflexi; Ktedonobacteria; Ktedonobacterales; Ktedonobacterales; Ktedonobacterales
Otu00118	interim	0.436	0.006	Bacteria; Chloroflexi; Ktedonobacteria; Ktedonobacteria; Ktedonobacteria; Ktedonobacteria
Otu00059	interim	0.462	0.002	Bacteria; Planctomycetes; Planctomycetia; Planctomycetales; Planctomycetaceae;
Otu00087	interim	0.426	0.001	Bacteria; Planctomycetes; Planctomycetia; Planctomycetales; Planctomycetaceae;
Otu00174	interim	0.447	0.006	Bacteria; Planctomycetes; Planctomycetia; Planctomycetales; Planctomycetaceae;
Otu00017	interim	0.400	0.001	Bacteria; Proteobacteria; Alphaproteobacteria; Rhizobiales;
Otu00148	interim	0.460	0.002	Bacteria; Proteobacteria; Alphaproteobacteria; Rhizobiales;
Otu00164	interim	0.560	0.006	Bacteria; Proteobacteria; Betaproteobacteria;
Otu00166	interim	0.477	0.001	Bacteria; Proteobacteria; Betaproteobacteria;
Otu00072	interim	0.482	0.001	Bacteria; Proteobacteria; Deltaproteobacteria;
Otu00137	interim	0.543	0.005	Bacteria; Proteobacteria; Deltaproteobacteria; Desulfuromonadales; Geobacteraceae; Geobacter
Otu00291	wet	0.932	0.001	Archaea; Euryarchaeota; Methanobacteria; Methanobacteriales; Methanobacteriaceae; Methanobacterium
Otu00068	wet	0.712	0.001	Bacteria; Acidobacteria; Acidobacteria Gp1;

Otu00171	wet	0.441	0.006	Bacteria; Acidobacteria; Acidobacteria Gp1;
Otu00231	wet	0.504	0.005	Bacteria; Acidobacteria; Acidobacteria Gp1;
Otu00238	wet	0.678	0.001	Bacteria; Acidobacteria; Acidobacteria Gp1;
Otu00003	wet	0.563	0.001	Bacteria; Acidobacteria; Acidobacteria Gp1;
Otu00008	wet	0.482	0.001	Bacteria; Acidobacteria; Acidobacteria Gp1;
Otu00012	wet	0.669	0.001	Bacteria; Acidobacteria; Acidobacteria Gp1;
Otu00063	wet	0.551	0.001	Bacteria; Acidobacteria; Acidobacteria Gp1;
Otu00124	wet	0.735	0.001	Bacteria; Acidobacteria; Acidobacteria Gp1;
Otu00140	wet	0.628	0.001	Bacteria; Acidobacteria; Acidobacteria Gp1;
Otu00187	wet	0.861	0.001	Bacteria; Acidobacteria; Acidobacteria Gp1;
Otu00303	wet	0.491	0.001	Bacteria; Acidobacteria; Acidobacteria Gp1;
Otu00060	wet	0.455	0.009	Bacteria; Acidobacteria; Acidobacteria Gp2;
Otu00180	wet	0.624	0.001	Bacteria; Acidobacteria; Acidobacteria Gp2;
Otu00033	wet	0.413	0.01	Bacteria; Acidobacteria; Acidobacteria Gp3;
Otu00088	wet	0.424	0.01	Bacteria; Actinobacteria; Actinobacteria;
Otu00191	wet	0.415	0.004	Bacteria; Actinobacteria; Actinobacteria; Actinomycetales;
Otu00044	wet	0.438	0.001	Bacteria; Actinobacteria; Actinobacteria; Actinomycetales; Thermomonosporaceae; Actinoallomurus
Otu00025	wet	0.484	0.001	Bacteria; Actinobacteria; Actinobacteria; Solirubrobacterales;
Otu00075	wet	0.627	0.001	Bacteria;
Otu00113	wet	0.563	0.001	Bacteria;
Otu00117	wet	0.723	0.001	Bacteria;
Otu00165	wet	0.626	0.001	Bacteria;
Otu00177	wet	0.523	0.006	Bacteria;
Otu00211	wet	0.846	0.001	Bacteria;
Otu00220	wet	0.570	0.002	Bacteria;
Otu00105	wet	0.588	0.001	Bacteria; Chloroflexi;
Otu00070	wet	0.461	0.001	Bacteria; Proteobacteria; Alphaproteobacteria; Alphaproteobacteria incertae sedis; Rhizomicrobium; Rhizomicrobium
Otu00052	wet	0.426	0.002	Bacteria; Proteobacteria; Alphaproteobacteria;
Otu00099	wet	0.428	0.006	Bacteria; Proteobacteria; Alphaproteobacteria; Rhizobiales; Hyphomicrobiaceae; Rhodomicrobium
Otu00119	wet	0.657	0.001	Bacteria; Proteobacteria; Alphaproteobacteria; Rhizobiales; Methylocystaceae; Methylocystis
Otu00036	wet	0.421	0.008	Bacteria; Proteobacteria; Alphaproteobacteria; Rhizobiales; Roseiarcaceae; Roseiarcus
Otu00080	wet	0.670	0.002	Bacteria; Proteobacteria; Deltaproteobacteria; Desulfuromonadales; Geobacteraceae; Geobacter
Otu00192	wet	0.508	0.006	Bacteria; Proteobacteria; Deltaproteobacteria; Desulfuromonadales; Geobacteraceae; Geobacter

Otu00189	wet	0.641	0.001	Bacteria; Proteobacteria; Deltaproteobacteria; Syntrophobacterales; Syntrophobacteraceae; Syntrophobacter
Otu00181	wet	0.615	0.001	Bacteria; Proteobacteria; Gammaproteobacteria;
Otu00149	wet	0.631	0.001	Bacteria; Verrucomicrobia; Subdivision3;
Otu00183	wet	0.839	0.001	Bacteria; Verrucomicrobia; Subdivision3;

References

Albuquerque, L., França, L., Rainey, F.A., Schumann, P., Nobre, M.F., Da Costa, M.S., 2011. Gaiella occulta gen. nov., sp. nov., a novel representative of a deep branching phylogenetic lineage within the class Actinobacteria and proposal of Gaiellaceae fam. nov. and Gaiellales ord. nov. Syst. Appl. Microbiol. 34, 595–599. https://doi.org/10.1016/j.syapm.2011.07.001

Apprill, A., Mcnally, S., Parsons, R., Weber, L., 2015. Minor revision to V4 region SSU rRNA 806R gene primer greatly increases detection of SAR11 bacterioplankton. Aquat. Microb. Ecol. 75, 129–137. https://doi.org/10.3354/ame01753

Ardón, M., Morse, J.L., Colman, B.P., Bernhardt, E.S., 2013. Drought-induced saltwater incursion leads to increased wetland nitrogen export. Glob. Chang. Biol. 19, 2976–2985. https://doi.org/10.1111/gcb.12287

Ardón, M., Morse, J.L., Doyle, M.W., Bernhardt, E.S., 2010. The Water Quality Consequences of Restoring Wetland Hydrology to a Large Agricultural Watershed in the Southeastern Coastal Plain. Ecosystems 13, 1060–1078. https://doi.org/10.1007/s10021-010-9374-x

Barton, K., 2019. Package "MuMIn."

Bates, D., Machler, M., Bolker, B., Walker, S., 2015. Fitting Linear Mixed-Effects Models Using lme4. J. Stat. Softw. 67, 1–48. https://doi.org/10.18637/jss.v067.i01

Boj, E., Caballe, A., Delicado, P., Fortiana, J., 2017. Package ' dbstats .'

Burgin, A.J., Yang, W.H., Hamilton, S.K., Silver, W.L., 2011. Beyond carbon and nitrogen: how the microbial energy economy couples elemental cycles in diverse ecosystems. Front. Ecol. Environ. 9, 44–52. https://doi.org/10.1890/090227

Caporaso, J.G., Lauber, C.L., Walters, W. a, Berg-Lyons, D., Huntley, J., Fierer, N., Owens, S.M., Betley, J., Fraser, L., Bauer, M., Gormley, N., Gilbert, J. a, Smith, G., Knight, R., 2012. Ultra-high-throughput microbial community analysis on the Illumina HiSeq and MiSeq platforms. ISME J. 6, 1621–1624. https://doi.org/10.1038/ismej.2012.8

Carmichael, M.J., Bernhardt, E.S., Bräuer, S.L., Smith, W.K., 2014. The role of vegetation in methane flux to the atmosphere: should vegetation be included as a distinct category in the global methane budget? Biogeochemistry 119, 1–24. https://doi.org/10.1007/s10533-014-9974-1

Chanton, J.P., 2005. The effect of gas transport on the isotope signature of methane in wetlands. Org. Geochem. 36, 753–768. https://doi.org/10.1016/j.orggeochem.2004.10.007

Conrad, R., 2009. The global methane cycle: recent advances in understanding the microbial processes involved. Environ. Microbiol. Rep. 1, 285–292. https://doi.org/10.1111/j.1758-2229.2009.00038.x

Davidson, N.C., Fluet-Chouinard, E., Finlayson, C.M., 2018. Global extent and distribution of wetlands: Trends and issues. Mar. Freshw. Res. 69, 620–627. https://doi.org/10.1071/MF17019

Fetzer, S., Bak, F., Conrad, R., 1993. Sensitivity of methanogenic bacteria from paddy soil to oxygen and desiccation. FEMS Microbiol. Ecol. 12, 107–115. https://doi.org/10.1111/j.1574-6941.1993.tb00022.x

Gorsky, A.L., Racanelli, G.A., Belvin, A.C., Chambers, R.M., 2019. Greenhouse gas flux from stormwater ponds in southeastern Virginia (USA). Anthropocene 28. https://doi.org/10.1016/j.ancene.2019.100218

Günther, A., Jurasinski, G., Huth, V., Glatzel, S., 2014. Opaque closed chambers underestimate methane fluxes of Phragmites australis (Cav.) Trin. ex Steud. Environ. Monit. Assess. 186, 2151–2158. https://doi.org/10.1007/s10661-013-3524-5

Hoffmann, M., Pehle, N., Huth, V., Jurisch, N., Sommer, M., Augustin, J., 2018. A simple method to assess the impact of sealing, headspace mixing and pressure vent on airtightness of manually closed chambers. J. Plant Nutr. Soil Sci. 181, 36–40. https://doi.org/10.1002/jpln.201600299

Hopfensperger, K.N., Burgin, A.J., Schoepfer, V.A., Helton, A.M., 2014. Impacts of Saltwater Incursion on Plant Communities, Anaerobic Microbial Metabolism, and Resulting Relationships in a Restored Freshwater Wetland. Ecosystems 17, 792–807. https://doi.org/10.1007/s10021-014-9760-x

Hu, Q., Cai, J., Yao, B., Wu, Q., Wang, Y., Xu, X., 2015. Plant-mediated methane and nitrous oxide fluxes from a carex meadow in Poyang Lake during drawdown periods. Plant Soil. https://doi.org/10.1007/s11104-015-2733-9

Hurvich, C., Tsai, C., 1993. A CORRECTED AKAIKE INFORMATIONON CRITERION FOR VECTOR AUTOREGRESSIVE MODEL SELECTION. J. Time Ser. Anal. 14, 271–279.

Jenkinson, B.J., Franzmeier, D.P., 2006. Development and Evaluation of Iron-Coated Tubes that Indicate Reduction in Soils. Soil Sci. Soc. Am. J. 70, 183–191. https://doi.org/10.2136/sssaj2004.0323

Kim, S.Y., Lee, S.H., Freeman, C., Fenner, N., Kang, H., 2008. Comparative analysis of soil microbial communities and their responses to the short-term drought in bog, fen, and riparian wetlands. Soil Biol. Biochem. 40, 2874–2880. https://doi.org/10.1016/j.soilbio.2008.08.004

Kozich, J.J., Westcott, S.L., Baxter, N.T., Highlander, S.K., Schloss, P.D., 2013. Development of a dual-index sequencing strategy and curation pipeline for analyzing amplicon sequence data on the miseq illumina sequencing platform. Appl. Environ. Microbiol. 79, 5112–5120. https://doi.org/10.1128/AEM.01043-13

Kuzyakov, Y., 2010. Soil Biology & Biochemistry Priming effects : Interactions between living and dead organic matter. Soil Biol. Biochem. 42, 1363–1371. https://doi.org/10.1016/j.soilbio.2010.04.003

Lennon, J.T., Jones, S.E., 2011. Microbial seed banks: The ecological and evolutionary implications of dormancy. Nat. Rev. Microbiol. 9, 119–130. https://doi.org/10.1038/nrmicro2504

Lew, S., Glińska-Lewczuk, K., 2018. Environmental controls on the abundance of methanotrophs and methanogens in peat bog lakes. Sci. Total Environ. 645, 1201–1211. https://doi.org/10.1016/j.scitotenv.2018.07.141

Luan, J., Wu, J., 2014. Gross photosynthesis explains the “artificial bias” of methane fluxes by static chamber (opaque versus transparent) at the hummocks in a boreal peatland. Environ. Res. Lett. 9. https://doi.org/10.1088/1748-9326/9/10/105005

McDonald, I.R., Murrell, J.C., 1997. The Methanol Dehydrogenase Structural Gene mxaF and Its Use as a Functional Gene Probe for Methanotrophs and Methylotrophs. FEMS Microbiol. Lett. 156, 205–

210.

Mehlich, A., 1984. Mehlich 3 Soil Test Extractant: A Modification of Mehlich 2 Extractant. Commun. Soil Sci. Plant Anal. 15, 1409–1416. https://doi.org/10.1080/00103628409367568

Mentzer, J.L., Goodman, R.M., Balser, T.C., 2006. Microbial response over time to hydrologic and fertilization treatments in a simulated wet prairie. Plant Soil 284, 85–100. https://doi.org/10.1007/s11104-006-0032-1

Millar, N., Urrea, A., Kahmark, K., Shcherbak, I., Robertson, G.P., Ortiz-Monasterio, I., 2018. Nitrous oxide (N2O) flux responds exponentially to nitrogen fertilizer in irrigated wheat in the Yaqui Valley, Mexico. Agric. Ecosyst. Environ. 261, 125–132. https://doi.org/10.1016/j.agee.2018.04.003

Mitsch, W.J., Bernal, B., Nahlik, A.M., Mander, Ü., Zhang, L., Anderson, C.J., Jørgensen, S.E., Brix, H., 2013. Wetlands, carbon, and climate change. Landsc. Ecol. 28, 583–597. https://doi.org/10.1007/s10980-012-9758-8

Mitsch, W.J., Gosslink, J.G., 2007. Wetlands, 4th ed. John Wiley & Sons, Hoboken.

Morse, J.L., Ardón, M., Bernhardt, E.S., 2012. Greenhouse gas fluxes in southeastern U.S. coastal plain wetlands under contrasting land uses. Ecol. Appl. 22, 264–280. https://doi.org/10.1890/11-0527.1

Mylavarapu, R., Obreza, T., Morgan, K., Hochmuth, G., Nair, V., Wright, A., 2014. Extraction of Soil Nutrients Using Mehlich-3 Reagent for Acid-Mineral Soils of Florida. Univ. Florida. Inst. Food Agric. Sci. 1–7.

Nygaard, B., Ejrnæs, R., 2009. The impact of hydrology and nutrients on species composition and richness: Evidence from a microcosm experiment. Wetlands 29, 187–195. https://doi.org/10.1672/08-13.1

Oksanen, J., 2015. Vegan : ecological diversity 1, 1–12. https://doi.org/10.1029/2006JF000545

Parada, A.E., Needham, D.M., Fuhrman, J.A., 2016. Every base matters: Assessing small subunit rRNA primers for marine microbiomes with mock communities, time series and global field samples. Environ. Microbiol. 18, 1403–1414. https://doi.org/10.1111/1462-2920.13023

Peralta, Ariane L, Ludmer, S., Matthews, J.W., Kent, A.D., 2014. Bacterial community response to changes in soil redox potential along a moisture gradient in restored wetlands. Ecol. Eng. 73, 246–253. https://doi.org/10.1016/j.ecoleng.2014.09.047

Peralta, Ariane L., Stuart, D., Kent, A.D., Lennon, J.T., 2014. A social-ecological framework for “micromanaging” microbial services. Front. Ecol. Environ. 12, 524–531. https://doi.org/10.1890/130308

Philippot, L., Raaijmakers, J.M., Lemanceau, P., Van Der Putten, W.H., 2013. Going back to the roots: The microbial ecology of the rhizosphere. Nat. Rev. Microbiol. 11, 789–799. https://doi.org/10.1038/nrmicro3109

Quast, C., Pruesse, E., Yilmaz, P., Gerken, J., Schweer, T., Yarza, P., Peplies, J., Glöckner, F.O., 2013. The SILVA ribosomal RNA gene database project: Improved data processing and web-based tools. Nucleic Acids Res. 41, 590–596. https://doi.org/10.1093/nar/gks1219

R Core Team, 2019. R: A language and environment for statistical computing. R Found. Stat. Comput. Vienna, Austria.

Rabenhorst, M.C., 2008. Protocol for Using and Interpreting IRIS Tubes. Soil Surv. Horizons 49, 74–77.

Roberts, D., 2016. Package ‘ labdsv .’

Rocca, J.D., Hall, E.K., Lennon, J.T., Evans, S.E., Waldrop, M.P., Cotner, J.B., Nemergut, D.R., Graham, E.B., Wallenstein, M.D., 2015. Relationships between protein-encoding gene abundance and corresponding process are commonly assumed yet rarely observed. ISME J. 9, 1693–9. https://doi.org/10.1038/ismej.2014.252

Rognes, T., Flouri, T., Nichols, B., Quince, C., Mahé, F., 2016. VSEARCH: a versatile open source tool for metagenomics. PeerJ 4, e2584. https://doi.org/10.7717/peerj.2584

Schloss, P.D., Westcott, S.L., Ryabin, T., Hall, J.R., Hartmann, M., Hollister, E.B., Lesniewski, R. a., Oakley, B.B., Parks, D.H., Robinson, C.J., Sahl, J.W., Stres, B., Thallinger, G.G., Van Horn, D.J., Weber, C.F., 2009. Introducing mothur: Open-source, platform-independent, community-supported software for describing and comparing microbial communities. Appl. Environ. Microbiol. 75, 7537–7541. https://doi.org/10.1128/AEM.01541-09

Schneider, C.A., Rasband, W.S., Eliceiri, K.W., 2012. NIH Image to ImageJ: 25 years of image analysis. Nat. Methods 9, 671–675. https://doi.org/10.1038/nmeth.2089

Sundberg, C., Jenny, J.S., Tonderski, K., Lindgren, P.E., 2007. Overland flow systems for treatment of landfill leachates-Potential nitrification and structure of the ammonia-oxidising bacterial community during a growing season. Soil Biol. Biochem. 39, 127–138. https://doi.org/10.1016/j.soilbio.2006.06.016

Truu, M., Juhanson, J., Truu, J., 2009. Microbial biomass, activity and community composition in constructed wetlands. Sci. Total Environ. 407, 3958–3971. https://doi.org/10.1016/j.scitotenv.2008.11.036